

Thermodynamics of Halogen Bonding in Solution: Substituent, Structural, and Solvent Effects

Mohammed G. Sarwar, Bojan Dragisic, Lee J. Salsberg, Christina Gouliaras, and
Mark S. Taylor*

Department of Chemistry, Lash Miller Chemical Laboratories, University of Toronto, Toronto,
Ontario M5S 3H6, Canada

Received October 10, 2009; E-mail: mtaylor@chem.utoronto.ca

Abstract: A detailed study of the thermodynamics of the halogen-bonding interaction in organic solution is presented. ^{19}F NMR titrations are used to determine association constants for the interactions of a variety of Lewis bases with fluorinated iodoalkanes and iodoarenes. Linear free energy relationships for the halogen bond donor ability of substituted iodoperfluoroarenes $\text{XC}_6\text{F}_4\text{I}$ are described, demonstrating that both substituent constants (σ) and calculated molecular electrostatic potential surfaces are useful for constructing such relationships. An electrostatic model is, however, limited in its ability to provide correlation with a more comprehensive data set in which both halogen bond donor and acceptor abilities are varied: the ability of computationally derived binding energies to accurately model such data is elucidated. Solvent effects also reveal limitations of a purely electrostatic depiction of halogen bonding and point to important differences between halogen bonding and hydrogen bonding.

Introduction

Halogen bonding (XB), the interaction between electron-deficient halogen compounds and electron donors, has emerged in recent years as a powerful and broadly useful noncovalent force relevant to such diverse fields as medicinal chemistry and organic materials (Figure 1).¹ Although the first systematic studies of halogen-bonding-based self-assembly were carried out decades ago,² it is only in recent years that chemists have begun to understand and exploit the full potential of this interaction. Metrangolo, Resnati, and co-workers have demonstrated convincingly that XB is a general strategy for crystal engineering and for the noncovalent assembly of new materials, sparking new levels of interest in this interaction. Halogen bonding has been employed for a wide range of applications, including liquid crystalline and magnetic materials, chiral discrimination, ion pair recognition, supramolecular polymer formation, porous material design, and chemical separation.³ The recognition that halogen-bonding interactions are surprisingly widespread in biological systems, and may hold consider-

able promise in medicinal chemistry, represents another significant development.⁴

Research reported over the past several years has provided considerable insight into the fundamental structural and energetic properties of the halogen-bonding interaction. The detailed investigations by Legon and co-workers of XB in the gas phase using rotational spectroscopy have provided a wealth of data, including geometries, directional preferences, and trends in binding energy.⁵ Numerous theoretical studies of XB have been undertaken,⁶ and it is generally accepted that the halogen-bonding interaction results from the “ σ -hole”,^{6j} a site of electron deficiency created when polarizable halogen atoms are bound to electronegative groups (Figure 1). Calculations suggest that

- (1) For reviews, see: (a) Metrangolo, P.; Meyer, F.; Pilati, T.; Resnati, G.; Terraneo, G. *Angew. Chem., Int. Ed.* **2008**, *47*, 6114–6127. (b) *Halogen Bonding: Fundamentals and Applications*; Metrangolo, P., Resnati, G., Eds.; Springer: Berlin, 2008. (c) Risannen, K. *Cryst. Eng. Commun.* **2008**, *10*, 1107–1113. (d) Politzer, P.; Lane, P.; Concha, M. C.; Ma, Y.; Murray, J. S. *J. Mol. Model.* **2007**, *13*, 305–311. (e) Metrangolo, P.; Neukirch, H.; Pilati, T.; Resnati, G. *Acc. Chem. Res.* **2005**, *38*, 386–395.
- (2) (a) Bent, H. A. *Chem. Rev.* **1968**, *68*, 587–648. (b) Hassel, O. *Science* **1970**, *170*, 497–502. (c) Dumas, J.-M.; Peurichard, H.; Gomel, M. J. *Chem. Res.* **1978**, 54–57.
- (3) For representative examples, see ref 1a and the following references: (a) Sun, A.; Goroff, N. S.; Lauher, J. W. *Science* **2006**, *312*, 1030–1034. (b) Nguyen, H. L.; Horton, P. N.; Hursthouse, M. B.; Legon, A. C.; Bruce, D. W. *J. Am. Chem. Soc.* **2004**, *125*, 16–17. (c) Metrangolo, P.; Carcenac, Y.; Lahtinen, M.; Pilati, T.; Rissanen, K.; Vij, A.; Resnati, G. *Science* **2009**, *323*, 1461–1464.

- (4) (a) Auffinger, P.; Hays, F. A.; Westhof, E.; Ho, P. S. *Proc. Natl. Acad. Sci. U.S.A.* **2004**, *101*, 16789–16794. (b) Trogdon, G.; Murray, J. S.; Concha, M. C.; Politzer, P. *J. Mol. Model.* **2007**, *13*, 313–318. (c) Voth, A. R.; Hays, F. A.; Ho, P. S. *Proc. Natl. Acad. Sci. U.S.A.* **2007**, *104*, 6188–6193. (d) Voth, A. R.; Khuu, P.; Oishi, K.; Ho, P. S. *Nat. Chem.* **2009**, *1*, 74–79.
- (5) Legon, A. C. *Angew. Chem., Int. Ed.* **1999**, *38*, 2686–2714.
- (6) For a review, see: (a) Karpfen, A. In ref 1b, pp 1–15. (b) Lommerse, J. P. M.; Stone, A. J.; Taylor, R.; Allen, F. H. *J. Am. Chem. Soc.* **1996**, *118*, 3108–3116. (c) Alkorta, I.; Rozas, J.; Elguero, J. *J. Phys. Chem. A* **1998**, *102*, 9278–9285. (d) Valerio, G.; Raos, G.; Meille, S. V.; Metrangolo, P.; Resnati, G. *J. Phys. Chem. A* **2000**, *104*, 1617–1620. (e) Karpfen, A. *J. Phys. Chem. A* **2000**, *104*, 6871–6879. (f) Wang, W. Z.; Wong, N.-B.; Zheng, W. X.; Tian, A. M. *J. Phys. Chem. A* **2004**, *108*, 1799–1805. (g) Zou, J. W.; Jian, Y. J.; Guo, M.; Hu, G. X.; Zhang, B.; Liu, H. C.; Yu, Q. S. *Chem.—Eur. J.* **2005**, *11*, 740–751. (h) Wang, Y. H.; Zou, J. W.; Lu, Y. X.; Yu, Q. S. *J. Theor. Comput. Chem.* **2006**, *4*, 719–721. (i) Riley, K. E.; Merz, K. M. *J. Phys. Chem. A* **2007**, *111*, 1688–1694. (j) Clark, T.; Hennemann, M.; Murray, J. S.; Politzer, P. *J. Mol. Model.* **2007**, *13*, 291–296. (k) Lu, Y.-X.; Zou, J.-W.; Wang, Y.-H.; Jiang, Y.-J.; Yu, Q.-S. *J. Phys. Chem. A* **2007**, *111*, 10781–10788. (l) Cavollotti, C.; Metrangolo, P.; Meyer, F.; Recupero, F.; Resnati, G. *J. Phys. Chem. A* **2008**, *112*, 9911–9918.

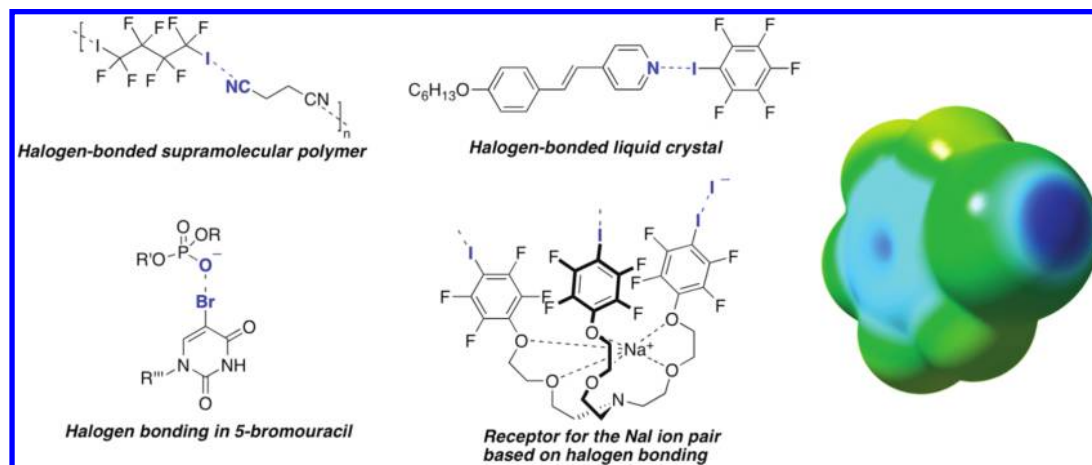


Figure 1. Representative applications of halogen bonding and a depiction of the molecular electrostatic potential of C_6F_5I demonstrating the “ σ -hole” at iodine (B3LYP/6-31+G**/LANLdp, Gaussian 03 (see the text for details); blue indicates a region of positive electrostatic potential).

the origin of the halogen-bonding interaction (electrostatic vs charge transfer) may depend on the structure of the components involved.^{6k}

Despite the progress achieved through the studies mentioned above, our understanding of XB remains limited in important respects. In particular, quantitative descriptions of halogen bonding in solution lag far behind those available for other noncovalent forces such as hydrogen bonding⁷ and interactions of π systems.⁸ Only a handful of association constants for halogen-bonding interactions in the solution phase have been determined.^{9–12} Data of this type are essential for developing and evaluating metrics for predicting the strength of halogen-bonding interactions. As a first step toward our long-term goal of applying halogen bonding for the development of new molecular receptors and catalysts, we have undertaken a systematic study of structural effects on the energies of halogen-bonding interactions. The goals of this study are (1) to determine the binding energies of halogen bond donor–acceptor pairs and (2) to evaluate the ability of empirically derived parameters (for example, substituent constants or solvent parameters) and computationally derived quantities to model trends in halogen

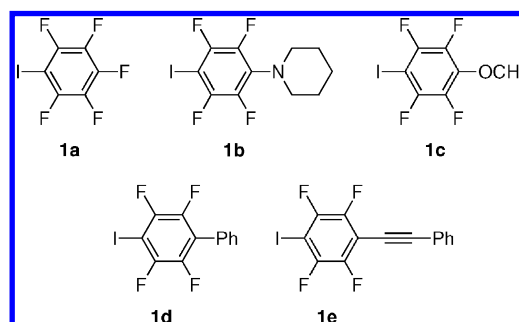


Figure 2. Structures of the substituted iodo-perfluoroarenes employed in the substituent effect study.

bond energies, with the aim of identifying quantities useful for predicting halogen-bonding affinities in solution. In addition to being important to our own research efforts, information of this type will be of value to emerging applications of halogen bonding in medicinal chemistry and materials design.

Results and Discussion

Experimental Determinations of K_a Values for Halogen-Bonding Interactions. Perfluorinated iodoalkanes and -arenes have been identified as among the strongest donors of halogen bonds (Figure 1). ^{19}F -NMR-based methods are ideally suited for probing halogen-bonding interactions of these species due to the high signal dispersion and sensitivity of ^{19}F NMR techniques. Metrangolo, Resnati, and co-workers have used ^{19}F NMR as the basis for a semiquantitative scale of halogen bond acceptor ability: the difference in chemical shift of the CF_2I group in a basic solvent of interest relative to that in a nonbasic (hydrocarbon) solvent is a measure of the acceptor ability of the solvent.¹³ Using ^{19}F NMR titrations, XB association constants for a number of donor–acceptor pairs have been determined by the Milan group^{11c} and by the groups of Brammer^{10b} and Hunter.^{11e} Results from this method are in agreement with data obtained by other means, including infrared and Raman spectroscopy, as well as calorimetric measurements. Likewise, we have found that this technique provides accurate

- (7) (a) Laurence, C.; Berthelot, M. *Perspect. Drug Discovery Des.* **2000**, *18*, 39–60. (b) Abraham, M. H.; Platts, J. A. *J. Org. Chem.* **2001**, *66*, 3484–3491. (c) Cook, J. L.; Hunter, C. A.; Low, C. M. R.; Perez-Velasco, A.; Vinter, J. G. *Angew. Chem., Int. Ed.* **2007**, *46*, 3706–3709.
- (8) Meyer, E. A.; Castellano, R. K.; Diederich, F. *Angew. Chem., Int. Ed.* **2003**, *42*, 1210–1250.
- (9) XB of haloalkynes: (a) Laurence, C.; Queignec-Cabanetos, M.; Dziembowska, T.; Queignec, R.; Wojtkowiak, B. *J. Chem. Soc. Perkin Trans. 2* **1982**, 1605–1610. (b) Laurence, C.; Queignec-Cabanetos, M.; Wojtkowiak, B. *Can. J. Chem.* **1983**, *61*, 135–138.
- (10) XB of haloarenes: (a) Wash, P. L.; Ma, S.; Obst, U.; Rebek, J. *J. Am. Chem. Soc.* **1999**, *121*, 7973–7974. (b) Libri, S.; Jasim, N. A.; Perutz, R. N.; Brammer, L. *J. Am. Chem. Soc.* **2008**, *130*, 7842–7844.
- (11) XB of haloalkanes: (a) Larsen, D. W.; Allred, A. L. *J. Phys. Chem.* **1965**, *69*, 2400–2401. (b) Blackstock, S. C.; Lorand, J. P.; Kochi, J. K. *J. Org. Chem.* **1987**, *52*, 1451–1460. (c) Metrangolo, P.; Panzeri, W.; Recupero, F.; Resnati, G. *J. Fluorine Chem.* **2002**, *114*, 27–33. (d) Rosokha, S. V.; Neretin, I. S.; Rosokha, T. Y.; Hecht, J.; Kochi, J. K. *Heteroat. Chem.* **2006**, *17*, 449–459. (e) Cabot, R.; Hunter, C. *Chem. Commun.* **2009**, 2005–2007.
- (12) In other studies, the relative acceptor abilities of bases or donor abilities of iodo compounds have been quantified by NMR or IR spectral changes, without measurement of association constants. See, for example: (a) Webb, J. A.; Klijn, J. E.; Hill, P. A.; Bennett, J. L.; Goroff, N. S. *J. Org. Chem.* **2004**, *69*, 660–664. (b) Laurence, C.; Queignec-Cabanetos, M.; Dziembowska, T.; Queignec, R.; Wojtkowiak, B. *J. Am. Chem. Soc.* **1981**, *103*, 2567–2573.

- (13) (a) Messina, M. T.; Metrangolo, P.; Panzeri, W.; Ragg, E.; Resnati, G. *Tetrahedron Lett.* **1998**, *39*, 9069–9072. (b) Lunghi, A.; Cardillo, P.; Messina, M. T.; Metrangolo, P.; Panzeri, W.; Resnati, G. *J. Fluorine Chem.* **1998**, *91*, 191–194.

Table 1. Halogen-Bonding Association Constants of *para*-Substituted Iodotetrafluorobenzenes (Tri-*n*-butylphosphine Oxide Acceptor, Cyclohexane Solvent), with Substituent Constants (σ_{para} and σ_{meta}) and Computed Values of the Molecular Electrostatic Potential Surface at the Iodine Atom

| substituent | K_a^a (M ⁻¹) | log K_a | σ_{para}^b | σ_{meta}^b | surface potential (AM1) ^d (kcal/mol) | surface potential (DFT) ^e (kcal/mol) |
|----------------------------------|----------------------------|-----------|--------------------|--------------------|---|---|
| F | 12 ± 2.5 | 1.0 | 0.06 | 0.34 | 24.2 | 25.8 |
| C≡CPh | 5.6 ± 1.1 | 0.75 | 0.16 | 0.14 | 20.8 | 22.9 |
| Ph | 3.9 ± 0.8 | 0.59 | -0.01 | 0.06 | 20.6 | 22.0 |
| OCH ₃ | 3.3 ± 0.7 | 0.52 | -0.27 | 0.12 | 20.7 | 22.5 |
| N(CH ₂) ₅ | 1.3 ± 0.3 | 0.11 | -0.83 ^c | -0.15 ^c | 20.0 | 18.9 |

^a Association constant K_a with tri-*n*-butylphosphine oxide in cyclohexane at 298 K determined by curve-fitting of ¹⁹F NMR titration data to a 1:1 binding isotherm. See the Supporting Information for full details. ^b Values of σ from Hansch, C.; Leo, A.; Unger, S. H.; Kim, K. H.; Nikaitani, D.; Lien, E. J. *J. Med. Chem.* **1973**, *16*, 1207–1216. ^c σ_{para} and σ_{meta} values for the dimethylamino substituent are listed. ^d Maximum value of the molecular electrostatic potential surface at the iodine atom, calculated at the AM1 level using Spartan 06. ^e Maximum value of the molecular electrostatic potential surface at the iodine atom, calculated at the DFT/B3LYP level of theory with the 6-31+G**·LANLdp basis set using Gaussian 03. See the text and Supporting Information for details.

and reproducible K_a determinations for halogen-bonding interactions of fluorinated aromatic and aliphatic organoiodides.

Titration curves were recorded by recording ¹⁹F NMR spectra of the halogen bond donor in the presence of increasing concentrations of acceptor: the signal corresponding to the fluorine atoms adjacent to the iodo substituent underwent a dramatic downfield shift upon increasing acceptor concentration, diagnostic of the halogen-bonding interaction.^{11c,e} The changes in chemical shift as a function of acceptor concentration were well-modeled by 1:1 binding isotherms using standard curve-fitting methods. All experiments described were carried out in duplicate or in triplicate and are reported with an estimated error of ±20% to reflect the weak nature of the interactions being studied.

Substituent Effects on the Halogen Bond Donor Ability of Iodoperfluorobenzenes. We began our investigation of substituent effects on XB by studying the effect of *para* substitution on the halogen bond donor ability of iodotetrafluorobenzenes (Figure 2). Linear free energy relationships based upon substituent effects represent a powerful tool for the study of noncovalent interactions. Insight into hydrogen-bonding,¹⁴ cation- π ,¹⁵ arene edge-face,¹⁶ and other interactions¹⁷ has been obtained through investigations of substituent effects. While Laurence and co-workers have shown that the strengths of halogen bonds involving substituted iodoacetylenes XC≡CI are linearly correlated with the Hammett substituent parameter σ ,^{9b} substituent effects on XB of haloarenes have not been reported to date.

We undertook measurements of the strengths of the halogen bonds of iodotetrafluorobenzenes **1a–1e** with a common acceptor, with the goal of evaluating the value of established substituent constants and computationally obtained quantities as predictors of XB donor ability. It should be noted that *para*-substituted iodotetrafluorobenzenes have been applied extensively as components of complex building blocks for crystal engineering, largely because of their ease of synthesis by nucleophilic aromatic substitution of iodopentafluorobenzene by

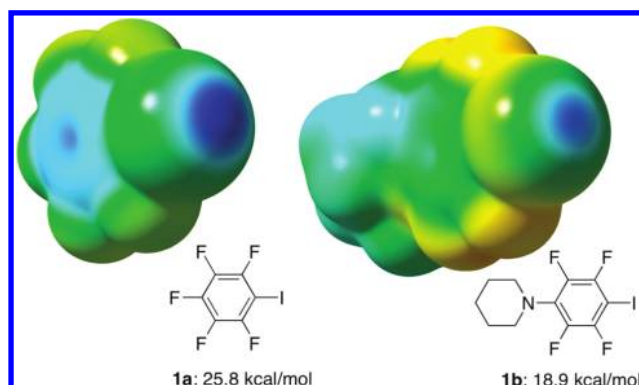


Figure 3. Molecular electrostatic potential surfaces (B3LYP/6-31+G**·LANLdp, Gaussian 03) of iodopentafluorobenzenes **1a** (left) and **1b** (right). Red indicates negative charge density and blue positive charge density: the plots have been set to the same color scale so that a visual comparison can be made. Maximum values of the surface electrostatic potential at the I atom are indicated beneath each structure.

alcohols or amines.¹⁸ Despite these widespread applications, the question of the electronic effect of a *para* oxygen or nitrogen substituent on the halogen bond donor ability of the C₆F₄I group has not been addressed.

Piperidine- and methoxy-substituted iodotetrafluorobenzenes **1b** and **1c** were prepared from iodopentafluorobenzene by nucleophilic aromatic substitution according to literature protocols.¹⁸ Halogen bond donors **1d**¹⁹ and **1e** were prepared from 1,4-diiodotetrafluorobenzene by palladium-catalyzed Sonogashira and Suzuki reactions, respectively. The association constants for the XC₆F₄I–tri-*n*-butylphosphine oxide (Bu₃PO) halogen bonds were determined in cyclohexane by ¹⁹F NMR as described above and are assembled in Table 1. As expected, the presence of electron-donating substituents (**1b**, **1c**) resulted in a lower halogen bond donor ability: the K_a value of **1a** is almost 10 times that of amine-substituted **1b**. Electrostatic potential surfaces of **1a** and **1b** show that the σ -hole, the site of electron deficiency at iodine where halogen bonding occurs, is considerably less pronounced upon introduction of the piperidine substituent (Figure 3).

A plot of log K_a vs the aromatic substituent constant σ shows a poor degree of correlation ($\rho = 0.74$, $r^2 = 0.82$, Figure 4a). The σ_{meta} constant frequently correlates well with phenomena that respond primarily to inductive/field effects,²⁰ and indeed

(14) (a) Wilcox, C. R.; Kim, E.; Romano, D.; Kuo, L. H.; Burt, A. L.; Curran, D. P. *Tetrahedron* **1995**, *51*, 621–634. (b) Deans, R.; Cooke, G.; Rotello, V. M. *J. Org. Chem.* **1997**, *62*, 836–839. (c) Deans, R.; Cuello, A. O.; Galow, T. H.; Ober, M.; Rotello, V. M. *J. Chem. Soc., Perkin Trans. 2* **2000**, 1309–1313.

(15) Zhong, W.; Gallivan, J. P.; Zhang, Y.; Li, L.; Lester, H. A.; Dougherty, D. A. *Proc. Natl. Acad. Sci. U.S.A.* **1998**, *95*, 12088–12093.

(16) (a) Carver, F. J.; Hunter, C. A.; Livingstone, D. J.; McCabe, J. F.; Seward, E. M. *Chem.—Eur. J.* **2002**, *8*, 2847–2859. (b) Kim, E.; Paliwal, S.; Wilcox, C. S. *J. Am. Chem. Soc.* **1998**, *120*, 11192–11193.

(17) Hof, F.; Scofield, D. M.; Schweizer, W. B.; Diederich, F. *Angew. Chem., Int. Ed.* **2004**, *43*, 5056–5059.

(18) Guardigli, C.; Liantonio, R.; Mele, M. L.; Metrangolo, P.; Resnati, G.; Pilati, T. *Supramol. Chem.* **2003**, *15*, 177–188.

(19) Collings, J. C.; Burke, J. M.; Smith, P. S.; Batsanov, A. S.; Howard, J. A. K.; Marder, T. B. *Org. Biomol. Chem.* **2004**, *2*, 3172–3178.

(20) Reynolds, W. F. *J. Chem. Soc., Perkin Trans. 1* **1980**, 985–992.

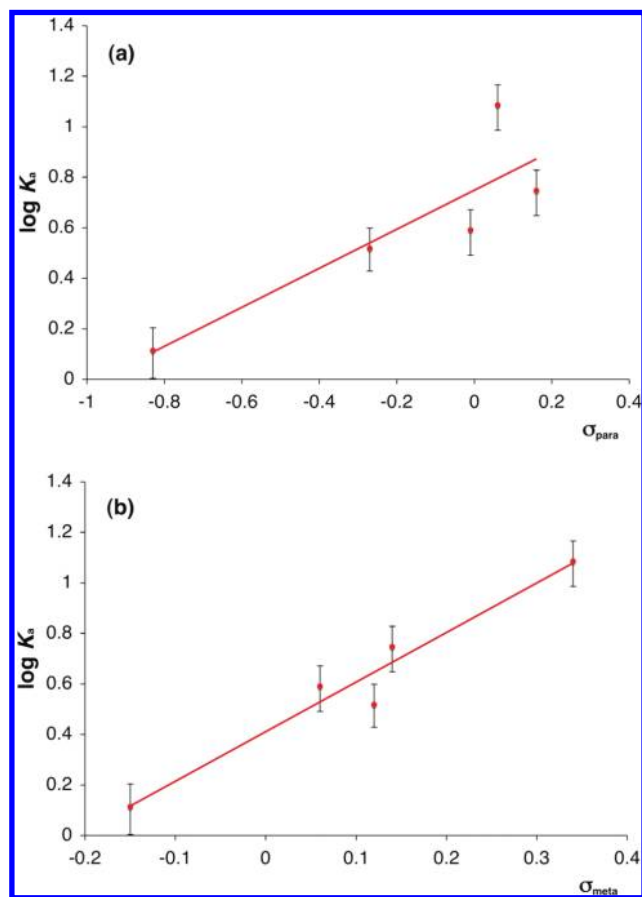


Figure 4. Correlation of the 4-X-C₆F₄I-Bu₃PO halogen bond strength log K_a with the (a) σ_{para} and (b) σ_{meta} substituent constants of X.

the plot of log K_a vs σ_{meta} shows a measurably higher correlation coefficient ($\rho = 1.8$, $r^2 = 0.94$, Figure 4b) than that of log K_a vs σ_{para} . These data are consistent with the idea that the effect of substituents on this halogen-bonding interaction is predominantly electrostatic in origin.

In search of more general predictors of trends in halogen-bonding ability, we turned to computational methods. It has been shown that the molecular electrostatic potential at a hydrogen atom of interest may be correlated with hydrogen bond donor ability^{14a,21,22} and that a similar calculation of potential at the centroid of an aryl group is a reliable measure of cation- π binding strength.²³ Given the low cost of such calculations, a similar relationship for halogen bonding could be valuable in the context of medicinal chemistry or in the design of new halogen bond donors. The relationship between molecular electrostatic potentials and the XB phenomenon has been discussed in some detail,^{4a,6j,24} and a recent computational study of acetone-bromoarene complexes revealed a linear relationship between calculated halogen-bonding energies and calculated

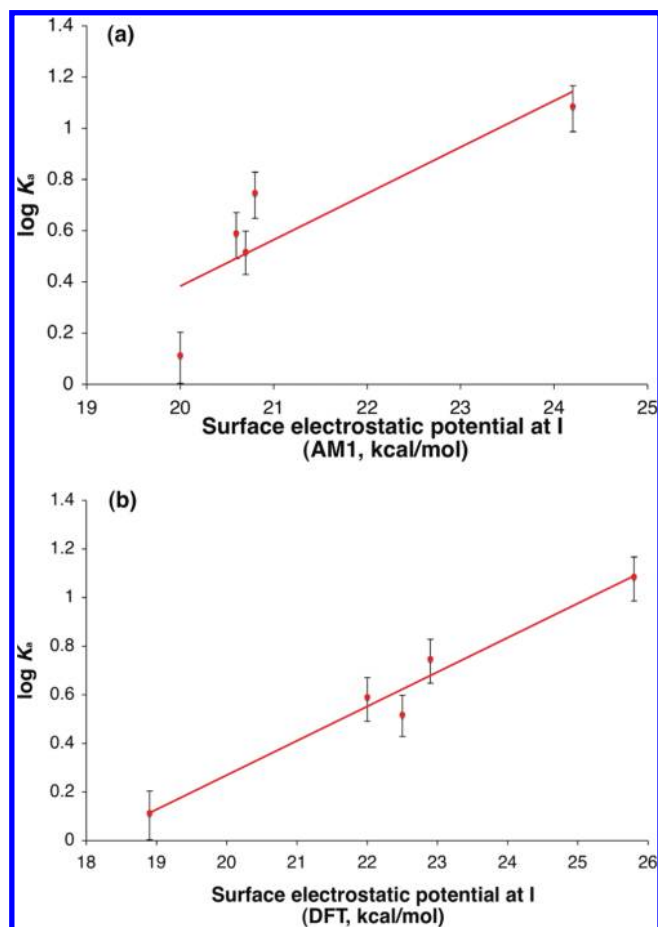


Figure 5. Correlation of the 4-X-C₆F₄I-Bu₃PO halogen bond strength log K_a with the electrostatic potential at the iodine atom, calculated with (a) AM1 and (b) DFT (B3LYP/6-31+G**·LANLdp) computational methods (see the text and Supporting Information).

electrostatic potential at the bromine atom.²⁵ However, *experiments* permitting quantitative correlations of calculated electrostatic potentials of halocarbons with measured XB thermodynamics have not been reported. Molecular electrostatic potential surfaces were calculated for **1a–1e** at the AM1 level of theory with Spartan 06, and the maximum values at the iodine atom are assembled in Table 1. These correlate poorly with the experimental binding energies ($r^2 = 0.73$, Figure 5a). Speculating that this poor degree of correlation might be a result of limitations of the ability of the AM1 semiempirical method to describe the electrostatic potential of iodoperfluoroarenes, we calculated the same quantity at a higher level of theory. Density functional theory (DFT) calculations were carried out with the B3LYP functional, using the 6-31+G** basis set for all atoms except iodine: the LANL2DZ effective core potential,²⁶ augmented with polarization functions of d symmetry and diffuse functions of p symmetry,²⁷ was employed for iodine. We denote this basis set 6-31+G**·LANLdp. Values of the electrostatic potential at iodine calculated at this level of theory provide excellent correlation with the experimental halogen bond donor abilities ($r^2 = 0.97$, Figure 5b).

(21) Hagelin, H.; Murray, J. S.; Brinck, T.; Berthelot, M.; Politzer, P. *Can. J. Chem.* **1995**, *73*, 483–488.

(22) (a) Deans, R.; Cooke, G.; Rotello, V. M. *J. Org. Chem.* **1997**, *62*, 836–839. (b) Deans, R.; Cuello, A. O.; Galow, T. H.; Ober, M.; Rotello, V. M. *J. Chem. Soc., Perkin Trans. 2* **2000**, 1309–1313.

(23) Mecozzi, S.; West, A. P., Jr.; Dougherty, D. A. *Proc. Natl. Acad. Sci. U.S.A.* **1996**, *93*, 10566–10571.

(24) Zordan, F.; Brammer, L.; Sherwood, P. J. *Am. Chem. Soc.* **2005**, *127*, 5979–5989.

(25) Riley, K. E.; Murray, J. S.; Politzer, P.; Concha, M. C.; Hobza, P. *J. Chem. Theory Comput.* **2009**, *5*, 155–163.

(26) Hay, P. J.; Wadt, W. R. *J. Chem. Phys.* **1985**, *82*, 270–283.

(27) Check, C. E.; Faust, T. O.; Bailey, J. M.; Wright, B. J.; Gilbert, T. M.; Sunderlin, L. S. *J. Phys. Chem. A* **2001**, *105*, 8111–8116.

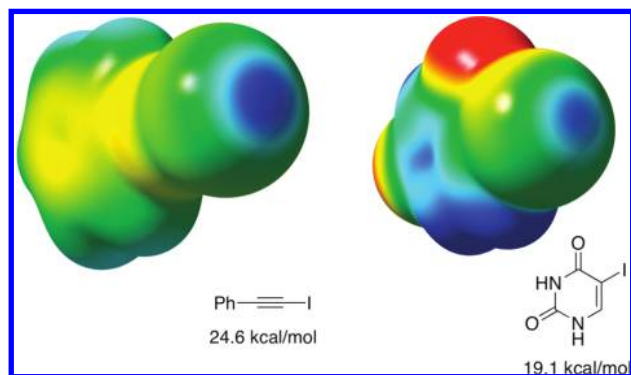


Figure 6. Molecular electrostatic potential surfaces (B3LYP/6-31+G**/LANLdp, Gaussian 03) of (iodoethynyl)benzene (left) and 5-iodoracil (right). Red indicates negative charge density and blue positive charge density: the plots have been set to the same color scale as those shown in Figure 3 so that a visual comparison can be made. Maximum values of the surface electrostatic potential at the I atom are indicated beneath each structure.

The experimental data described above confirm that molecular electrostatic potentials calculated at an appropriate level of theory are of considerable value in predicting the relative strengths of halogen-bonding interactions, in agreement with the computational work of the Politzer group.^{6j} We calculated electrostatic potential surfaces for two compounds known to form halogen bonds: (iodoethynyl)benzene, a representative alkynyl iodide of the type studied by the groups of Laurence⁹ and Goroff,^{3a,12a} and 5-iodoracil, a halogenated nucleobase of the type that forms XB in biological systems (Figure 6).^{4a} At the level of theory described above, the maximum values of the σ -hole for these compounds are 24.6 and 19.1 kcal/mol, respectively. These fall within the range of values explored in this substituent effect study and suggest that, to a first approximation, these structurally distinct organohalides may have halogen bond donor ability similar to that of the compounds studied in detail here.

Structural Effects on Halogen Bonding: A Combined Experimental and Computational Approach. The data discussed above demonstrate that, within the series of substituted iodoperfluoroaromatics **1a–1e**, the effect of substituents on halogen bond donor ability is well-modeled by electrostatic effects. This observation suggests that the model of Hunter and co-workers,²⁸ which uses pairwise electrostatic effects as the basis for accurate

(28) For a review, see: Hunter, C. A. *Angew. Chem., Int. Ed.* **2004**, *43*, 5310–5324. In brief, the Hunter model treats noncovalent interactions in solution as a competition between pairwise electrostatic interactions of solute and solvent molecules. Solvents and solutes are characterized by donor ability α and acceptor ability β . The values of α and β are obtained either from experimental measurements of hydrogen-bonding association constants or from molecular electrostatic potential calculations. The latter are generally carried out at the AM1 level, and the resulting maximum and minimum values of the electrostatic potential surface E_{\max} and E_{\min} are used to estimate α and β using the following equations:

$$\alpha = E_{\max}/(52 \text{ kJ/mol}) \quad (1)$$

$$\beta = E_{\min}/(52 \text{ kJ/mol}) \quad (2)$$

The energy of interaction of donor X and acceptor Y in solvent S is estimated by the following equation

$$\Delta G = -(\alpha_X - \alpha_S)(\beta_Y - \beta_S) + 6 \text{ kJ/mol} \quad (3)$$

where α_X is the donor ability of X, α_S is the donor ability of the solvent, β_Y is the acceptor ability of Y, and β_S is the acceptor ability of the solvent. The cost of bringing two molecules together in solution is estimated to be 6 kJ/mol.

Table 2. Experimental and Predicted Binding Energies of C_6F_5I and $C_8F_{17}I$ with Representative Halogen Bond Acceptors

| halogen bond ^a | K_a^b (M^{-1}) | ΔG^c (kcal/mol) | predicted ΔG^d (kcal/mol) |
|----------------------------|----------------------|-------------------------|-----------------------------------|
| $C_6F_5I-Et_3N$ | 1.3 ± 0.2 | -0.2 ± 0.1 | 0.3 |
| $C_6F_5I-Bu_2SO$ | 2.0 ± 0.4 | -0.4 ± 0.1 | 0.1 |
| $C_8F_{17}I-Et_3N$ | 2.8 ± 0.6 | -0.6 ± 0.1 | -0.7 |
| $C_8F_{17}I-Bu_2SO$ | 6.2 ± 1.2 | -1.1 ± 0.1 | -1.1 |
| $C_6F_5I-Bu_3PO$ | 12 ± 2.5 | -1.5 ± 0.1 | -0.2 |
| $C_8F_{17}I-Bu_3PO$ | 18 ± 4 | -1.7 ± 0.1 | -1.6 |
| C_6F_5I -quinuclidine | 20 ± 4 | -1.8 ± 0.1 | 0 |
| $C_8F_{17}I$ -quinuclidine | 34 ± 7 | -2.1 ± 0.1 | -1.2 |

^a Halogen bond acceptors are abbreviated as follows: Et_3N = triethylamine; Bu_2SO = di-*n*-butyl sulfoxide; Bu_3PO = tri-*n*-butylphosphine oxide. ^b Association constant K_a in cyclohexane at 298 K, determined by curve-fitting of ¹⁹F NMR titration data to a 1:1 binding isotherm. ^c Free energy of binding calculated from the association constant. ^d Free energy of binding predicted by the Hunter pairwise electrostatic interaction model (see the text).

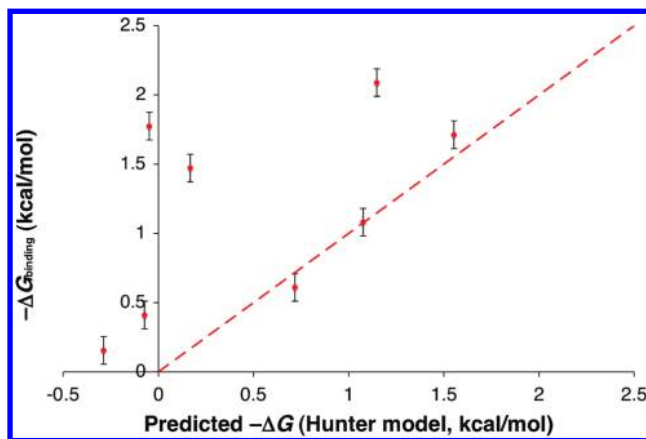


Figure 7. Experimental binding data ($-\Delta G_{\text{binding}}$) against values predicted by the model of Hunter and co-workers. The dotted line represents $y = x$.

predictions of noncovalent bond energies in solution, may be useful as a predictive tool for halogen bonding. Indeed, the Hunter group recently measured the strengths of the halogen bonds of iodoperfluorohexane with a variety of Lewis bases in three solvents and showed that their electrostatic model, as well as other parameters including donor nucleophilicity, correlated quite well with the experimental data.^{11e} While the relative contributions of electrostatic, charge-transfer, and dispersion components to XB continue to be debated, computational studies generally suggest that the charge-transfer and dispersion components may not be negligible, particularly as the strengths of the interactions are varied. It is thus unclear to what extent a purely electrostatic model should be useful for predicting the association constants of halogen bonds involving partners that vary widely in structure.

To probe this issue, we took a distinct approach from that of Hunter and co-workers by selecting two different halogen bond donors (iodoperfluorooctane and iodopentafluorobenzene) and measuring the strengths of their interactions with four electronically distinct electron donors (triethylamine, di-*n*-butyl sulfoxide, tri-*n*-butylphosphine oxide, and quinuclidine) in cyclohexane. The binding data are assembled in Table 2.

A plot of the eight experimentally determined free energies of binding against those predicted by the Hunter model is shown in Figure 7. The predicted values in cyclohexane (Table 2) were obtained using parameters for hydrocarbon solvents ($\alpha = 1.2$ and $\beta = 0.6$) developed recently by Hunter and co-workers.²⁹

These parameters are based on determinations of a large set of hydrogen-bonding association constants in nonpolar solvents. While the magnitudes of the free energies of binding are predicted quite successfully, the correlation between the predicted and experimental values is poor ($r^2 = 0.3$). Values of β suggest that XB acceptor ability should decrease in the order $\text{Bu}_3\text{PO} > \text{Bu}_2\text{SO} \sim \text{quinuclidine} > \text{Et}_3\text{N}$, whereas the experimental acceptor abilities follow the order $\text{quinuclidine} > \text{Bu}_3\text{PO} > \text{Me}_2\text{SO} > \text{Et}_3\text{N}$. We note that assigning values of α to the halogen bond donors is not straightforward: the predictions in Table 2 are based on values derived from AM1 electrostatic potential surfaces for consistency with Hunter's approach ($\alpha = 1.9$ for $\text{C}_6\text{F}_5\text{I}$ and 2.5 for $\text{C}_8\text{F}_{17}\text{I}$). However, our substituent effect studies (see the previous section) indicate that charge distributions in iodoperfluorocarbons are not accurately described by this semiempirical method. DFT calculations suggest values of α for $\text{C}_6\text{F}_5\text{I}$ and $\text{C}_8\text{F}_{17}\text{I}$ of 2.1 and 2.0 , respectively. These parameters provide poorer correlation still with experimental data because they improperly order the donor abilities of the two compounds.

In search of approaches that would provide better predictive power for the thermodynamics of halogen bonding, we turned to gas-phase calculations of binding energies. Halogen bonding has been the subject of many computational studies, and both DFT and MP2 calculations (particularly the latter) have been shown to model the experimental geometries and spectral properties^{61,30} of XB complexes with good accuracy. On the other hand, systematic comparisons of computationally predicted halogen-bonding energies with experimental data are lacking: this is a reflection of the small set of experimental binding data available to date. The accuracy with which computational methods are able to describe noncovalent interactions is the subject of much active research,^{31,32} and XB represents an interesting test case because it may differ from hydrogen bonding in terms of the importance of electrostatic, charge-transfer, and dispersion contributions. Moreover, identifying calculated quantities with the predictive power of the thermodynamics of XB has clear practical relevance.

For the purposes of time efficiency, truncated models of the halogen-bonded complexes shown in Table 2 were used in the computational studies: $\text{C}_8\text{F}_{17}\text{I}$ was simplified to $\text{C}_4\text{F}_9\text{I}$, dibutyl sulfide to dimethyl sulfide, and tributylphosphine oxide to trimethylphosphine oxide. Geometry optimizations of the XB complexes were first carried out using DFT (B3LYP), with the 6-31+G***-LANLdp* basis described in the previous section. The gas-phase binding energies (ΔE_{B3LYP}) of the complexes were obtained by subtracting the sum of the calculated energies of the isolated components from the calculated energy of the complex. Corrections for the basis set superposition error were carried out by the counterpoise (CP) method of Boys and Bernardi:³³ counterpoise-corrected binding energies are denoted $\Delta E_{\text{B3LYP}}^{\text{CP}}$. The calculated results are assembled in Table 3.³⁴

A plot of the experimental free energies of binding ($-\Delta G_{\text{binding}}$, Table 2) against the counterpoise-corrected B3LYP 6-31+G**-

Table 3. Computed Halogen-Bonding Energies for Comparison to Experimental Data From Table 2

| halogen bond ^a | $\Delta E_{\text{B3LYP}}^b$ (kcal/mol) | $\Delta E_{\text{B3LYP}}^{\text{CP}c}$ (kcal/mol) |
|---|--|---|
| $\text{C}_6\text{F}_5\text{I}-\text{Et}_3\text{N}$ | -2.0 | -1.3 |
| $\text{C}_6\text{F}_5\text{I}-\text{Me}_2\text{SO}$ | -2.9 | -2.5 |
| $\text{C}_4\text{F}_9\text{I}-\text{Et}_3\text{N}$ | -2.5 | -2.1 |
| $\text{C}_4\text{F}_9\text{I}-\text{Me}_2\text{SO}$ | -3.4 | -2.9 |
| $\text{C}_6\text{F}_5\text{I}-\text{Me}_3\text{PO}$ | -3.6 | -3.1 |
| $\text{C}_4\text{F}_9\text{I}-\text{Me}_3\text{PO}$ | -4.0 | -3.6 |
| $\text{C}_6\text{F}_5\text{I}-\text{quinuclidine}$ | -4.4 | -3.8 |
| $\text{C}_4\text{F}_9\text{I}-\text{quinuclidine}$ | -3.5 | -3.3 |

^a Halogen bond acceptors are abbreviated as follows: Et_3N = triethylamine; Me_2SO = dimethyl sulfoxide; Me_3PO = trimethylphosphine oxide. ^b DFT-calculated (B3LYP/6-31+G***-LANLdp*) binding energy (see above and the Supporting Information). ^c DFT-calculated binding energy, corrected for the basis set superposition error by the CP method (see the text).

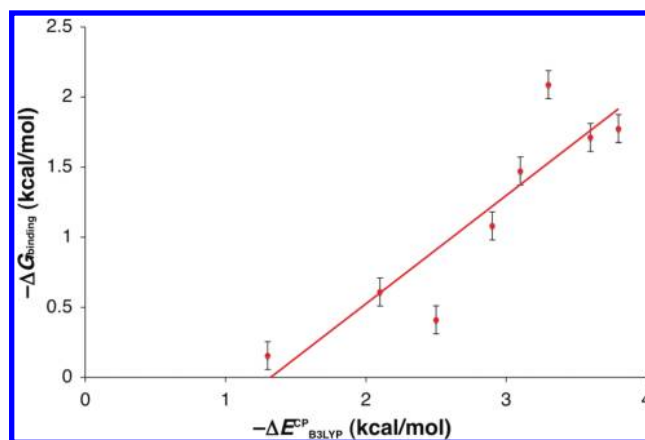


Figure 8. Experimental binding data ($-\Delta G_{\text{binding}}$, Table 2) against DFT-calculated ($-\Delta E_{\text{B3LYP}}^{\text{CP}}$, Table 3) gas-phase binding energy.

LANLdp binding energies of the corresponding simplified complexes ($-\Delta E_{\text{B3LYP}}^{\text{CP}}$, Table 3) is shown in Figure 8. Given that limitations of the B3LYP functional have been identified in terms of its ability to model energies and geometries of noncovalent interactions in general,³² and halogen-bonding interactions in particular,²⁵ the agreement between calculated and experimental binding data is perhaps surprisingly good. The DFT calculations systematically predict binding energies higher than those measured experimentally, but correspondence between these two sets of data is not to be expected given the fundamental differences between the computed gas-phase energies of interaction (which were not corrected for zero-point-energy differences here) and the free energy changes measured in solution. Nonetheless, there is a significant correlation between calculated and experimental data ($r^2 = 0.81$). The interaction posing the most significant problem for this level of theory is the strongest association studied (the $\text{C}_8\text{F}_{17}\text{I}$ -quinuclidine halogen bond): this point lies significantly above the trendline shown in Figure 8. Previous work by Lu and co-workers suggests that a covalent contribution to halogen bonding becomes important as the strengths of these interactions increase;^{6k} similar models for hydrogen bonding have been put forward by Gilli and co-workers.³⁵ We speculate that the strong quinuclidine-iodoperfluoroalkane halogen bond may involve a contribution from charge-transfer, dispersion, or covalent character that

(29) Cabot, R.; Hunter, C. A.; Varley, L. M. *Org. Biomol. Chem.*, in press.

(30) (a) Rege, P. D.; Malkina, O. L.; Goroff, N. S. *J. Am. Chem. Soc.* **2002**, *124*, 370–371. (b) Glaser, R.; Chen, N.; Wu, H.; Knotts, N.; Kaupp, M. *J. Am. Chem. Soc.* **2004**, *126*, 4412–4419.

(31) Müller-Dethlefs, K.; Hobza, P. *Chem. Rev.* **2000**, *100*, 143–167.

(32) Zhao, Y.; Truhlar, D. G. *J. Chem. Theory Comput.* **2005**, *1*, 415–432, and references therein.

(33) Boys, S. F.; Bernardi, F. *Mol. Phys.* **1970**, *19*, 553.

(34) Zero-point-energy-corrected binding energies were also calculated and provide poorer correlation with the experimental data. See the Supporting Information.

(35) Gilli, P.; Bertolasi, V.; Ferretti, V.; Gilli, G. *J. Am. Chem. Soc.* **1994**, *116*, 909–915.

is not well-modeled by DFT with the B3LYP functional.³² Hunter and co-workers also noted the failure of their electrostatic model to accurately predict the halogen-bonding energies of strong acceptors such as quinuclidine.^{11e} Higher level calculations are under way to shed light on this point. However, we note that, with the exception of the C₈F₁₇I–quinuclidine pair, B3LYP/6-31+G**/LANLdp calculations show useful degrees of correlation with experimental data and may be useful in guiding the design of new halogen-bonding motifs.

Solvent Effects on Halogen Bonding. The solvent dependence of noncovalent interactions is of considerable interest: not only are fundamental properties of an interaction revealed by its medium dependence, but the information gathered from such studies is also valuable as a predictive tool for applications in self-assembly or medicinal chemistry. While solvent effects on hydrogen bonding,^{7c,36} aromatic edge–face and face–face interactions,³⁷ and other noncovalent forces have been analyzed in detail, studies of solvent effects on halogen bonding remain limited in comparison. Laurence and co-workers noted that the association between pyridine and 1-cyano-2-iodoacetylene is more favorable in carbon tetrachloride than in benzene solution,^{9b} and the group of Kochi observed that K_a values for the CBr₄–DABCO complex followed the trend CHCl₃ > CH₃CN > CH₃OH.^{11b} These small data sets do not enable correlation of halogen bond strengths with known metrics of solvent properties. In their recent study, Hunter and co-workers measured the strengths of halogen-bonding interactions of iodoperfluorohexane with a variety of donors in three solvents, chloroform, benzene, and carbon tetrachloride, and obtained data that were largely consistent with their electrostatic model of noncovalent interactions (see above).^{11e} While this data set was useful in evaluating this specific model, it represents a limited selection of commonly employed solvents and does not allow comparisons to other, empirically developed solvent scales in current use. In particular, Lewis basic donor solvents were not investigated.

We thus assembled a complementary set of data, measuring the association constants for a single XB interaction (iodoperfluorooctane–triethylamine) in 10 diverse solvents. Association constants in methanol and dimethyl sulfoxide were too low to be determined by NMR, while those in chloroform and 2-propanol represent the lower limits of the NMR technique. For the range of solvents for which accurate determinations of K_a were possible, the iodoperfluorooctane–triethylamine association constant showed a detectable variation in magnitude (Table 4).

A graph of the experimental binding data ($\log K_a$) against the predictions of the Hunter electrostatic model is shown

Table 4. Association Constants for the Iodoperfluorooctane–Triethylamine Complex in Various Solvents as a Function of the Solvent Properties

| solvent | K_a^a (M ⁻¹) | $\log K_a$ | $E_T(30)^b$ (kcal/mol) | py ^c |
|----------------------------|----------------------------|------------|------------------------|-----------------|
| cyclohexane | 2.8 ± 0.6 | 0.45 | 31 | 0.58 |
| benzene | 2.6 ± 0.5 | 0.41 | 34 | 1.05 |
| acetonitrile | 1.9 ± 0.4 | 0.20 | 46 | 1.79 |
| dichloromethane | 1.8 ± 0.3 | 0.20 | 41 | 1.35 |
| acetone | 1.3 ± 0.3 | 0.11 | 42 | 1.64 |
| tetrahydrofuran | 1.2 ± 0.2 | 0.08 | 37 | 1.35 |
| dioxane | 1.1 ± 0.2 | 0.04 | 36 | 1.5 |
| <i>tert</i> -butyl alcohol | 0.7 ± 0.3 | −0.15 | 43 | 0.92 |
| chloroform | 0.6 ± 0.4 | −0.2 | 35 | 1.25 |
| 2-propanol | 0.3 ± 0.7 | −0.4 | 48 | 1.09 |

^a Association constant K_a for the Et₃N–IC₈F₁₇ halogen bond (298 K) obtained by curve-fitting ¹⁹F NMR titration data to a 1:1 binding isotherm. ^b Values of $E_T(30)$ from ref 39. ^c Values of py from ref 40.

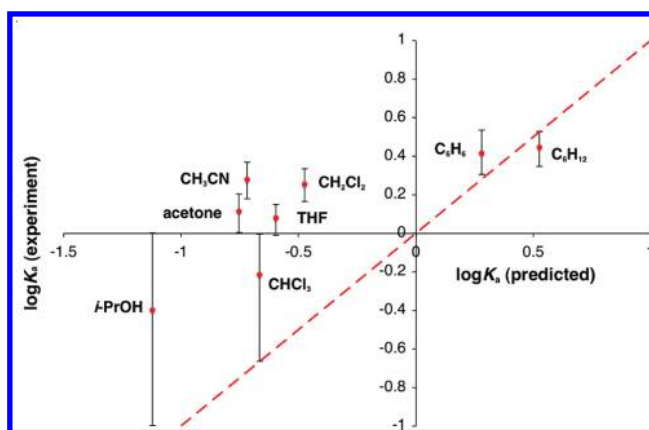


Figure 9. Experimental binding data ($\log K_a$ for the C₈F₁₇I–triethylamine interaction) plotted against binding data predicted by the Hunter electrostatic model. The dotted line represents $y = x$.

in Figure 9.³⁸ In agreement with previous results,^{11e} the data for chloroform and benzene lie on the line $y = x$ within experimental error, as do those for cyclohexane and 2-propanol. However, the situation is dramatically different in the case of the Lewis basic solvents acetone, acetonitrile, and tetrahydrofuran. In all three cases, the experimental binding constants are significantly higher than the predicted values. *The triethylamine–iodoperfluorooctane interaction is more favorable in competitive, Lewis basic solvents than is predicted by an electrostatic model.* Whether this behavior results from limitations of the description of the Et₃N–IC₈F₁₇ halogen bond as a purely electrostatic interaction, the unusual solubility properties of the perfluoroalkanes, or some other phenomenon is not clear. Nonetheless, this observation may be important in applications of halogen bonding in solution, particularly where competition with other types of interactions is a concern.

A traditional way to characterize solvent effects on noncovalent interactions is to employ empirically developed solvent polarity parameters.³⁹ We found that graphs of $\log K_a$ against values of commonly used polarity scales such as $E_T(30)$ (Figure 10a) and π^* (see the Supporting Information) led to a common conclusion: the Et₃N–IC₈F₁₇ interaction shows a relatively minor response to solvent polarity within the range of solvents tested, but is significantly weakened in solvents that can serve as competitive hydrogen bond donors. The py scale, based on the intensities of vibronic bands of pyrene fluorescence, illustrates this point well (Figure 10b): while many solvent scales that employ solvatochromic dyes—including $E_T(30)$ —actually

- (36) Beeson, C.; Pham, N.; Shipps, G., Jr.; Dix, T. A. *J. Am. Chem. Soc.* **1993**, *115*, 6803–6812, and references cited therein.
- (37) (a) Cockroft, S. L.; Hunter, C. A. *Chem. Commun.* **2006**, 3806–3808. (b) Cubberley, M. S.; Iverson, B. L. *J. Am. Chem. Soc.* **2001**, *123*, 7560–7563. (c) Breault, G. A.; Hunter, C. A.; Mayers, P. C. *J. Am. Chem. Soc.* **1998**, *120*, 3402–3410. (d) Smithrud, D. B.; Diederich, F. *J. Am. Chem. Soc.* **1990**, *112*, 339–343.
- (38) The values of $\alpha = 2.5$ for iodoperfluorooctane and $\beta = 7.5$ for triethylamine reported in ref 11d were used. Values of α and β reported in ref 7c were used for acetonitrile, acetone, tetrahydrofuran, and chloroform. New parameters developed by Hunter and co-workers (ref 29) were employed for cyclohexane ($\alpha = 1.2$, $\beta = 0.6$), benzene ($\alpha = 1.1$, $\beta = 1.6$), and dichloromethane ($\alpha = 1.7$, $\beta = 1.5$). Values for 2-propanol ($\alpha = 2.7$, $\beta = 5.5$) were provided by Prof. C. A. Hunter (personal communication).
- (39) Reichardt, C. *Solvents and Solvent Effects in Organic Chemistry*, 3rd ed.; Wiley-VCH: Weinheim, Germany, 2003.
- (40) Dong, D. C.; Winnik, M. *Can. J. Chem.* **1984**, *62*, 2560–2565.

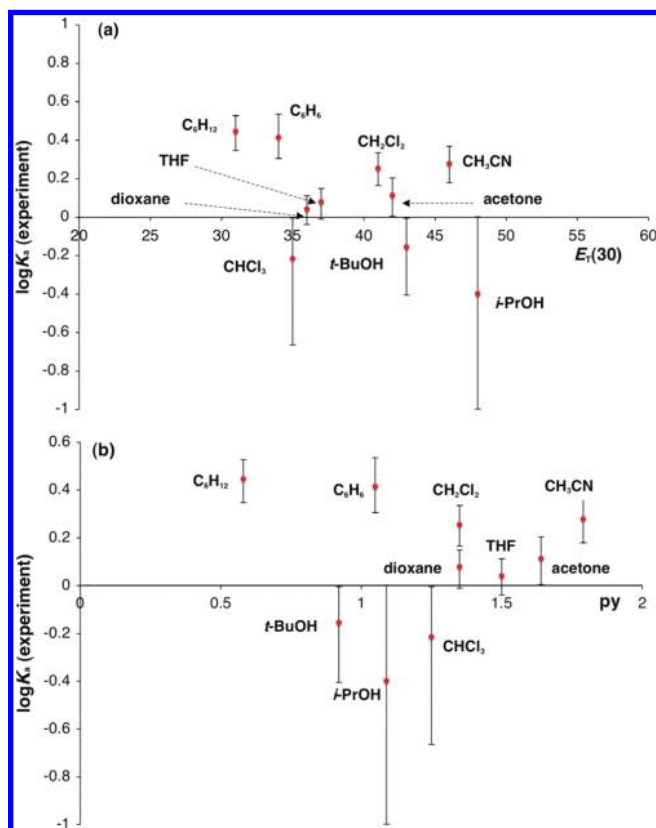


Figure 10. Experimental binding data ($\log K_a$ for the $C_8F_{17}I$ –triethylamine interaction) as a function of solvent polarity as measured by (a) $E_T(30)$ and (b) the py scale.

measure a combination of polarity and hydrogen bond donor ability, the py scale quite efficiently separates these effects, providing a measure of polarity without a substantial H bond donor contribution.⁴⁰ The hydrogen bond donor solvents *tert*-butyl alcohol, chloroform, and 2-propanol are clear outliers from a data set that otherwise shows relatively minor variation of the strength of the halogen-bonding interaction as a function of py . These data suggest that hydrogen bond donor solvents are able to compete with iodoperfluoroalkane for binding to the common acceptor triethylamine. Competition between halogen bond and hydrogen bond donors for a common acceptor has also been observed in the solid state.⁴¹

Conclusions

We have measured association constants for the relatively strong halogen bonds of iodoperfluoroalkanes and iodoperfluoroarenes employed most frequently in modern applications of the XB interaction. When the electronic properties of a halogen

bond donor are varied in a systematic, incremental fashion—as in the measurements of the interactions of *para*-substituted iodoperfluoroarenes presented here—electrostatic models may be of significant value. The fact that XB interactions are subject to linear free energy relationships with empirically derived substituent parameters (σ) and quantities derived from calculations (molecular electrostatic potentials) represents a basis for systematically tuning halogen bond donor ability in the context of receptor or drug design.

A wider variation of the structure of halogen-bonding partners also reveals limits to a purely electrostatic approach: a data set that includes interaction energies of two halogen bond donors with four halogen bond acceptors that vary widely in structure is poorly modeled by an electrostatic model. Instead, DFT-calculated binding constants show moderate correlation with experimental data, except in the case of the strongest halogen bond of the data set (quinclidine–iodoperfluoroalkane). This represents the most extensive comparison of experimentally determined halogen bond energies with computed data to date, and it demonstrates that DFT methods may have utility in modeling the types of halogen bonds currently applied in supramolecular settings. It also will represent a useful data set for testing the ability of newer DFT functionals and higher level calculations to describe trends in the thermodynamics of halogen bonding.

Limitations to an electrostatic model are also revealed through studies of solvent effects: while hydrogen bond donor solvents are detrimental to XB in solution, Lewis basic solvents compete with triethylamine for halogen bonds less well than would be expected on the basis of electrostatic interactions alone. Thus, while this study provides support for the characterization of XB as an interaction with a dominant electrostatic component, it also reveals subtle differences between this interaction and hydrogen bonding. These differences may represent interesting opportunities for exploiting halogen bonding in competition or cooperation with other noncovalent interactions.

Acknowledgment. This work was supported by NSERC (Discovery Grants Program), the Canadian Foundation for Innovation (Leaders Opportunity Fund), the Ontario Ministry of Research and Innovation (Research Infrastructure Program), the University of Toronto, and Merck Research Laboratories (Canadian Academic Development Program). We thank Prof. Mitch Winnik for his advice and valuable comments on this study and Prof. Datong Song for assistance with the DFT calculations. We also thank Prof. Chris Hunter (Department of Chemistry, University of Sheffield) for helpful discussions and for sharing unpublished data on new values of α and β for nonpolar solvents.

Supporting Information Available: Complete experimental procedures, data analysis, and computational details. This material is available free of charge via the Internet at <http://pubs.acs.org>.

JA9086352

(41) (a) Metrangolo, P.; Resnati, G. *Science* **2008**, *321*, 918–919. (b) Corradi, E.; Meille, S. V.; Messina, M. T.; Metrangolo, P.; Resnati, G. *Angew. Chem., Int. Ed.* **2000**, *39*, 1782–1785. (c) Aakeröy, C. B.; Fasulo, M.; Schultheiss, N.; Desper, J.; Moore, C. *J. Am. Chem. Soc.* **2007**, *129*, 13772–13773.